Pergamon

Geochimica et Cosmochimica Acta, Vol. 67, No. 7, pp. 1375–1382, 2003

0016-7037/03 $30.00 + .00

doi:10.1016/S0016-7037(02)01296-6

Model for kinetic effects on calcium isotope fractionation (δ^{44}Ca) in inorganic aragonite and cultured planktonic foraminifera

NIKOLAUS GUSSONE,[1] ANTON EISENHAUER,[1,*] ALEXANDER HEUSER,[1,2] MARTIN DIETZEL,[3] BARBARA BOCK,[1] FLORIAN BÖHM,[1] HOWARD J. SPERO,[4] DAVID W. LEA,[5] JELLE BIJMA,[6] and THOMAS F. NÄGLER[7]

[1]GEOMAR, Forschungszentrum für Marine Geowissenschaften, Wischhofstr. 1-3, D-24148 Kiel, Germany
[2]Graduierten Kolleg "Dynamik globaler Kreisläufe im System Erde," GEOMAR Forschungszentrum für marine Geowissenschaften, Wischhofstr. 1-3, 24148 Kiel, Germany
[3]Institut für Technische Geologie und Angewandte Mineralogie, Technische Universität Graz, A-8010 Graz, Rechbauerstrasse 12, Austria
[4]Department of Geology, University of California, Davis, One Shield Avenue, Davis, CA 95616, USA
[5]Department of Geological Sciences, University of California, Santa Barbara, CA 93106, USA
[6]Alfred Wegener Institut für Polar und Meeresforschung, Kolumbuskai 1, D-27515 Bremerhaven, Germany
[7]Isotopengeologie, Mineralogisch-petrographisches Institut, Universität Bern, Erlachstrasse 9a, CH-3012 Bern, Switzerland

(*Received January* 28, 2002; *accepted in revised form October* 4, 2002)

Abstract—The calcium isotope ratios ($\delta^{44}Ca = [(^{44}Ca/^{40}Ca)_{sample}/(^{44}Ca/^{40}Ca)_{standard} - 1] \cdot 1000$) of *Orbulina universa* and of inorganically precipitated aragonite are positively correlated to temperature. The slopes of 0.019 and 0.015‰ $°C^{-1}$, respectively, are a factor of 13 and 16 times smaller than the previously determined fractionation from a second foraminifera, *Globigerinoides sacculifer*, having a slope of about 0.24‰ $°C^{-1}$. The observation that δ^{44}Ca is positively correlated to temperature is opposite in sign to the oxygen isotopic fractionation ($\delta^{18}O$) in calcium carbonate ($CaCO_3$). These observations are explained by a model which considers that Ca^{2+}-ions forming ionic bonds are affected by kinetic fractionation only, whereas covalently bound atoms like oxygen are affected by kinetic and equilibrium fractionation. From thermodynamic consideration of kinetic isotope fractionation, it can be shown that the slope of the enrichment factor α(T) is mass-dependent. However, for *O. universa* and the inorganic precipitates, the calculated mass of about 520 ± 60 and 640 ± 70 amu (atomic mass units) is not compatible with the expected ion mass for ^{40}Ca and ^{44}Ca. To reconcile this discrepancy, we propose that Ca diffusion and δ^{44}Ca isotope fractionation at liquid/solid transitions involves Ca^{2+}-aquocomplexes ($Ca[H_2O]_n^{2+} \cdot mH_2O$) rather than pure Ca^{2+}-ion diffusion. From our measurements we calculate that such a hypothesized Ca^{2+}-aquocomplex correlates to a hydration number of up to 25 water molecules (490 amu). For *O. universa* we propose that their biologically mediated Ca isotope fractionation resembles fractionation during inorganic precipitation of $CaCO_3$ in seawater. To explain the different Ca isotope fractionation in *O. universa* and in *G. sacculifer*, we suggest that the latter species actively dehydrates the Ca^{2+}-aquocomplex before calcification takes place. The very different temperature response of Ca isotopes in the two species suggests that the use of δ^{44}Ca as a temperature proxy will require careful study of species effects.

1. INTRODUCTION

The important role of calcium (Ca) in biologic processes is based on its chemical versatility, which is related to its highly adaptable coordination geometry, its divalent charge, modest binding energies, fast reaction kinetics, and its inertness in redox reactions (Williams, 1989; Williams, 1974). It was suggested that changes in the calcium concentration, together with changes in seawater alkalinity and pH, were a major driving force for the onset of biomineralization and the alternating mineralogy of marine carbonate precipitation observed throughout Earth's history. However, there are only a few data sets that link seawater concentrations or calcium isotope ratios to Earth's biologic evolution (De La Rocha and DePaolo, 2000; Arp et al., 2001; Wallmann, 2001; Stanley and Hardie, 1998; Kempe and Degens, 1985; Degens, 1979). Natural fractionation of Ca isotopes in surface processes is reported to be relatively small (Heumann et al., 1970; Heumann and Lieser, 1972; Heumann et al., 1982; Stahl and Wendt, 1968) requiring high analytical precision to be resolved. Russell et al. (1978) first combined modern high-precision mass spectrometry with the application of the Ca double spike technique to determine isotope fractionation in terrestrial and cosmic materials. Skulan et al. (1997, 1999) focused their attention on the biologic control of the Ca isotopic composition. They analyzed Ca from various marine organisms and concluded that Ca isotope fractionation is relatively uniform in magnitude among vastly different organisms and that Ca becomes isotopically lighter when it moves through food chains. Zhu and MacDougall (1998) suggested that Ca isotope data from foraminifera of a given species may significantly vary with ocean water temperature or depth and showed that there is a 0.6‰ difference in the δ^{44}Ca ratios between *G. sacculifer* from the Holocene and the last glacial maximum (LGM) of the equatorial Pacific (Zhu and MacDougall, 1998). Utilizing recent estimates of sea surface temperature change since the last glacial maximum (Lea et al., 2000), this 0.6‰ difference would reflect a temperature change of ~3°C. A more systematic study of δ^{44}Ca–temperature relationships in the cultured planktonic foraminifera *Globigerinoides sacculifer* demonstrated a clear temperature dependence over a temperature range from 19.5 to 29.5°C (Nägler et al.,

* Author to whom correspondence should be addressed (aeisenhauer@geomar.de).

2000). The calculated δ^{44}Ca–temperature slope of ~0.24‰ °C^{-1} was similar to the observations of Zhu and MacDougall (1998). Further, Nägler et al. (2000) found a 0.7‰ difference in δ^{44}Ca of fossil *G. sacculifer* between Holocene and LGM core sections of equatorial Atlantic core GeoB1112. Thus, a significant temperature dependence of δ^{44}Ca has been established for *G. sacculifer*. The magnitude of the temperature sensitivity is similar to that for oxygen isotope ratios (δ^{18}O), although the positive slope for δ^{44}Ca is opposite in sign compared to other stable isotope systems such as oxygen (O), carbon (C), and boron (B) where isotope fractionation is inversely related to temperature (Zeebe and Wolf-Gladrow, 2001).

In a further study, De La Rocha and DePaolo (2000) used an intertidal benthic foraminifer, *Glabratella ornatissima*, to establish a δ^{44}Ca–temperature relationship. Although the authors claim that this species does not display a temperature relationship, in our opinion the small temperature range (8.5 to 10.8°C) used for calibration and the scatter of their data do not allow for a definitive conclusion.

The discrepant statements concerning temperature-controlled δ^{44}Ca isotope fractionation reflect the absence of a thermodynamic model describing temperature-dependent inorganic or biologically mediated δ^{44}Ca fractionation. To address this problem, we systematically investigated the temperature-dependent δ^{44}Ca fractionation of inorganically precipitated aragonite and of another cultured planktonic foraminifera, *O. universa*, and compared the results with the earlier measurements on cultured *G. sacculifer*.

2. MATERIAL AND METHODS

2.1. Inorganic Precipitation of Aragonite: Experimental Setup

The setup for inorganic precipitation of aragonite is described in detail in Dietzel and Usdowski (1996). The experimental setup consists of two bottles: a 0.5-L polyethylene (PE) bottle, containing 35 g solid $NaHCO_3$ which is saturated with CO_2 gas from a tank with a pressure of 1 atm. The inner bottle is surrounded by a 5-L container filled with a Ca-Mg-Cl solution (Ca: 0.01 mol L^{-1}; Mg: 0.02 mol L^{-1}) and selected trace metals. The concentrations of Ca, Mg, and Cl and the Ca: Mg: Cl ratios in the solutions used for the inorganic precipitation of aragonite were chosen to gain pure aragonite precipitation and are different from modern seawater. In particular, the solutions contained no sulfate, although in seawater ~10% of the solved Ca is complexed by sulfate ions. The issue here is to gather first-order information on the kinetics of inorganic Ca isotope fractionation and its temperature dependence, rather than to investigate the complexities of the open ocean environment. Reagent grade chemicals (Merck p.a.) and pure gases (Messer-Griesheim CO_2: 99.995 vol.%) were used for the experiments. Only ~2% of the dissolved Ca was precipitated, so that the isotopic composition and concentration of Ca remained nearly constant during the experiment.

When CO_2 diffuses through the PE walls, $CaCO_3$ precipitates as aragonite within the Ca-Mg-Cl solution. Each experiment was terminated when ~100 mg of $CaCO_3$ were precipitated. At temperatures of 10°C and 50°C (±0.3°C), ~20 d and ~2 d were needed for the precipitation of ~100 mg aragonite, respectively. The aragonite was grown at a pH of 9.0, which was kept constant during the entire experiment to prevent the formation of brucite. The entire experiment was carried out in an inert N_2-atmosphere. After termination of each experiment, the precipitated solids were removed from the outer solution by filtration through a 0.2-μm membrane filter under nitrogen atmosphere. Some additional solids were mechanically removed from the outside of the 0.5-L bottle. The solids were washed with double distilled water until the remaining solution was chloride-free and dried at 30°C. The mineralogical composition of the solids was identified by X-ray diffraction (goniometer type Philips PW 1130/1370) and infrared spectroscopy (Perkin Elmer FTIR 1600) at the University of Göttingen, Germany.

2.2. Culture Experiments (*O. universa*)

Foraminifers were maintained in laboratory cultures between 10.5°C and 29.3°C (±0.2°C) at either the Wrigley Institute for Environmental Science on Santa Catalina Island (California, USA) or at the Isla Magueyes Marine Laboratory on Puerto Rico. *Orbulina universa* were collected by scuba divers and were grown in 0.8 μm filtered sea water using standard procedures (Spero, 1998; Spero et al., 1997). All analyzed specimens were collected as "juvenile" presphere individuals. The complete precipitation of the spherical chamber which was used for δ^{44}Ca analysis occurred under controlled conditions in the laboratory. For the temperature calibration, *O. universa* were cultured in ambient seawater. The pH drops with increasing temperature due to the temperature-dependent dissociation constants. However, the pH values varied only between ~8.1 and 8.3. For studying the effect of CO_3^{2-} changes on the δ^{44}Ca, *O. universa* was cultured at 22°C in seawater containing 137 to 530 μmol kg^{-1} CO_3^{2-}.

2.3. Sample Preparation and δ^{44}Ca Measurements

For determination of the Ca isotope composition ~1 mg of aragonite or 5 to 40 μg of foraminiferal test calcite were dissolved in 2.5N ultrapure HCl. An isotopically well-defined ^{43}Ca/^{48}Ca double spike was added to an aliquot of the solution to correct for isotope fractionation in the mass spectrometer during the course of the Ca isotope analysis. The sample–spike mixture was dried and recovered in ~2 μL 2.5N HCl and then loaded with a Ta_2O_5-activator solution using the "sandwich-technique" (activator-sample-activator) onto a previously outgassed single filament (zone refined rhenium). After evaporating to dryness, the filament with the sample/spike mixture was briefly glowed.

Measurements of the isotopic composition of Ca were performed on a Finnigan MAT 262 RPQ$^+$ thermal ionization mass spectrometer at GEOMAR research center in Kiel, Germany. The mass spectrometer was operated in positive ionization mode with a 10-kV acceleration voltage and a 10^{11} Ω resistor for the faraday cups. A stable ion-beam of ~3 to 5 V on mass 40 is achieved at ~1550 to 1580°C. Data acquisition is performed in two steps because the dispersion of our mass spectrometer does not account for the mass range from 40 to 48 atomic mass units (amu). In the first step, masses 40, 41, 42, 43 and in a second step 44 and 48 are measured simultaneously. During data acquisition ^{41}K was continuously monitored for correction of isobaric interferences on mass 40, although we found that this interference or any other possible isobaric interferences are negligible. To calculate the "true" ^{44}Ca/^{40}Ca ratio of the carbonate sample, the measured isotope ratios have to be corrected for the added ^{43}Ca/^{48}Ca double spike. This correction is carried out using the mathematical algorithm of Compston and Oversby (1969) slightly modified by adopting an exponential mass fractionation law. The isotope variations of Ca are expressed as δ^{44}Ca values ($\delta^{44}\text{Ca} = [(^{44}\text{Ca}/^{40}\text{Ca})_{\text{sample}}/(^{44}\text{Ca}/^{40}\text{Ca})_{\text{standard}} - 1]*1000$), where the measured ^{44}Ca/^{40}Ca ratios are normalized relative to the ^{44}Ca/^{40}Ca ratio of a CaF_2 standard solution (^{44}Ca/^{40}Ca: 0.021208; Russell et al., 1978). Such a normalization procedure was previously used by Nägler et al. (2000) and Russell et al. (1978). More details of our analytical method are given in Heuser et al. (2002). To monitor our long-term reproducibility, we repeatedly measured two internal standards, natural CaF_2 and calcium carbonate (NIST SRM915a). Our 95 measurements of the CaF_2 standard show a mean ^{44}Ca/^{40}Ca ratio of 0.0212594 ± 0.0000005 ($2\sigma_m$). All measurements of samples and standard materials are normalized to this value. As our ^{43}Ca/^{48}Ca double spike is not calibrated for the determination of the absolute ^{44}Ca/^{40}Ca ratio, the above values do not represent the true isotopic composition of the CaF_2 standard. One hundred five measurements of NIST SRM915a show a mean δ^{44}Ca value of −1.450 ± 0.025‰ ($2\sigma_m$). The mean 2σ reproducibility of our samples is ~0.12‰ (ranging from 0.03 to 0.2‰) determined by repeated aliquot measurements of various sample materials. To improve the statistical significance of a single δ^{44}Ca measurement, all samples were measured at least twice.

3. RESULTS

The δ^{44}Ca values of *O. universa* and the inorganically precipitated aragonite are presented in Table 1. From Figure 1 it can be seen that the values of the inorganic precipitates and of *O. universa* are generally lower than their corresponding bulk solution. Furthermore, the δ^{44}Ca ratios of all carbonates are positively correlated to temperature although the temperature sensitivity of the previously measured *G. sacculifer* (Nägler et al., 2000) is a factor of ~13 and 16, respectively, larger than that of *O. universa* and the precipitates.

Precipitates:

$$\delta^{44}Ca_{arag} = 0.015 \cdot T(°C) - 2.23 : \delta^{44}Ca_{fluid} = -0.3‰ \quad (1)$$

O. universa:

$$\delta^{44}Ca_{calcite} = 0.019 \cdot T(°C) - 0.96 : \delta^{44}Ca_{fluid} = 0.5‰ \quad (2)$$

G. sacculifer:

$$\delta^{44}Ca_{calcite} = 0.24 \cdot T(°C) - 8.00 : \delta^{44}Ca_{fluid} = 0.5‰ \quad (3)$$

In contrast to the δ^{18}O system which becomes isotopically lighter with increasing temperature, the δ^{44}Ca values increase with increasing temperature (Fig. 2).

Figure 3 shows the enrichment factors of *G. sacculifer*, *O. universa*, and the aragonite as a function of the inverse temperature [$\alpha(T) = (^{44}Ca/^{40}Ca)_{fluid}/(^{44}Ca/^{40}Ca)_{solid}$]. From logarithmic fits to our isotope and temperature data, the calculated initial enrichment factors α_0 and slopes (ζ) are presented in Table 2 and discussed below.

To investigate the influence of the $(CO_3)^{2-}$ concentration on the Ca isotope fractionation, we cultured *O. universa* at 22°C in seawater containing $(CO_3)^{2-}$ concentrations between 137 and 530 μmol kg^{-1}. Figure 4 shows that our data do not show any significant relationship between the $(CO_3)^{2-}$ concentration (and hence pH) and the corresponding δ^{44}Ca values in *O. universa.*

4. DISCUSSION

4.1. Calcium Diffusion and Isotope Fractionation

To understand the opposite fractionation behavior of the $^{18}O/^{16}O$ and the $^{44}Ca/^{40}Ca$ isotope systems, two possible isotope fractionation processes have to be taken into account: (1) equilibrium isotope fractionation due to the vibrational characteristics of the light and heavy isotopes related to covalent atomic bonding, and (2) kinetic isotope fractionation due to the different transport reaction characteristics of light and heavy isotopes during diffusion across the boundary layer between a solution and a solid (O'Neil, 1986; O'Neil et al., 1969; Bigeleisen and Mayer, 1947; Urey, 1947). Kinetic isotope fractionation occurs at any boundary layer from one phase to another (e.g., liquid/solid, liquid/enzyme) because lighter isotopes always tend to diffuse faster than heavier isotopes which results in an enrichment of the lighter isotopes in the product phase. In contrast, equilibrium fractionation occurs as a consequence of covalent atomic bonding. During molecule formation the incorporation of heavier isotopes is preferred because covalent atomic bonds formed with heavier isotopes show larger

Table 1. δ^{44}Ca values of cultured *O. universa* and inorganically grown aragonite

Sample	T °C	δ^{44}Ca ($CaCO_3$)	α(T)	CO_3^{2-} (μmol · kg^{-1})	Light
O. universa	10.5	−0.71	1.00121	amb	
O. universa	10.5	−0.73	1.00123	amb	
O. universa	12.9	−0.69	1.00119	amb	
O. universa	12.9	−0.74	1.00124	amb	
O. universa	16.2	−0.72	1.00122	amb	
O. universa	18	−0.63	1.00113	amb	
O. universa	18	−0.65	1.00115	amb	
O. universa	21	−0.58	1.00108		hl
O. universa	21	−0.69	1.00119		hl
O. universa	22	−0.57	1.00107	156	
O. universa	23.3	−0.56	1.00106	amb	hl
O. universa	23.3	−0.46	1.00096	amb	hl
O. universa	27	−0.44	1.00094	amb	hl
O. universa	27	−0.40	1.00090	amb	hl
O. universa	27	−0.45	1.00095	amb	hl
O. universa	29.2	−0.64	1.00114	190	hl
O. universa	29.3	−0.33	1.00083		hl
O. universa	29.3	−0.36	1.00086		hl
O. universa	29.3	−0.41	1.00091		hl
O. universa	29.3	−0.46	1.00096		ll
O. universa	29.3	−0.43	1.00093		ll
O. universa	22	−0.54	1.00104	324	
O. universa	22	−0.58	1.00108	260	
O. universa	22	−0.64	1.00114	242	
O. universa	22	−0.70	1.00120	242	
O. universa	22	−0.46	1.00096	324	
O. universa	22	−0.54	1.00104	220	
O. universa	22	−0.58	1.00108	220	
O. universa	22	−0.65	1.00115	530	
O. universa	22	−0.55	1.00105	137	
Aragonite	10	−2.07	1.00178		
Aragonite	10	−2.10	1.00180		
Aragonite	10	−2.18	1.00188		
Aragonite	10	−2.01	1.00171		
Aragonite	19	−1.94	1.00164		
Aragonite	19	−1.91	1.00162		
Aragonite	19	−1.98	1.00168		
Aragonite	30	−1.83	1.00153		
Aragonite	30	−1.81	1.00152		
Aragonite	30	−1.77	1.00147		
Aragonite	30	−1.73	1.00143		
Aragonite	30	−1.84	1.00154		
Aragonite	30	−1.86	1.00156		
Aragonite	30	−1.68	1.00138		
Aragonite	30	−1.72	1.00142		
Aragonite	40	−1.54	1.00124		
Aragonite	40	−1.62	1.00132		
Aragonite	40	−1.60	1.00130		
Aragonite	40	−1.61	1.00131		
Aragonite	40	−1.60	1.00130		
Aragonite	40	−1.65	1.00135		
Aragonite	50	−1.54	1.00125		
Aragonite	50	−1.52	1.00123		
Aragonite	50	−1.58	1.00128		
Aragonite	50	−1.46	1.00116		
Aragonite	50	−1.43	1.00113		
Aragonite	50	−1.57	1.00128		
Aragonite	50	−1.58	1.00128		

δ^{44}Ca value of the seawater was determined to be 0.5‰. The δ^{44}Ca for the bulk solution ($CaCl_2$) of the aragonite was determined to be −0.3‰.

hl = high light; ll = low light; amb = ambient CO_3^{2-} content of seawater.

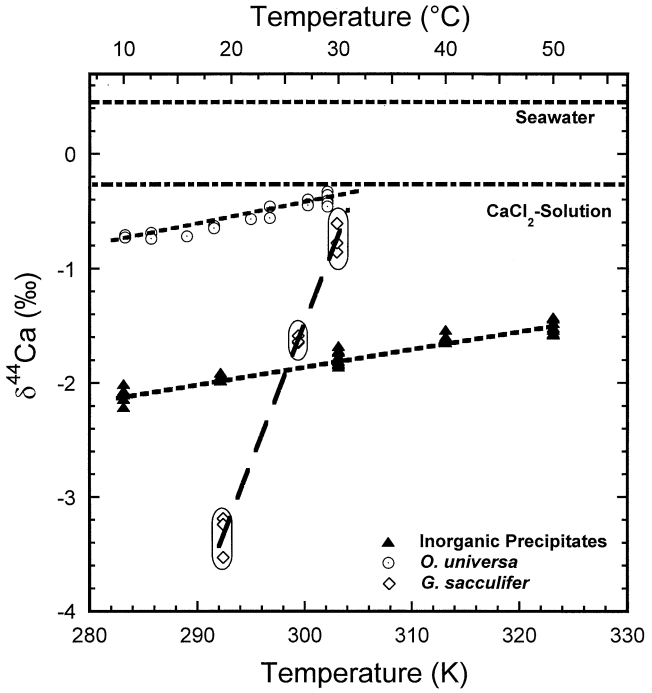

Fig. 1. The δ^{44}Ca values of the inorganic precipitates and *O. universa* correlate with temperature. All carbonate samples are isotopically lighter than the corresponding bulk solution from which they precipitated. For comparison we show the δ^{44}Ca values for *G. sacculifer* (Nägler et al., 2000). The δ^{44}Ca ratios of *G. sacculifer* show a 13 and 16 times steeper slope than *O. universa* and the inorganic precipitates, respectively.

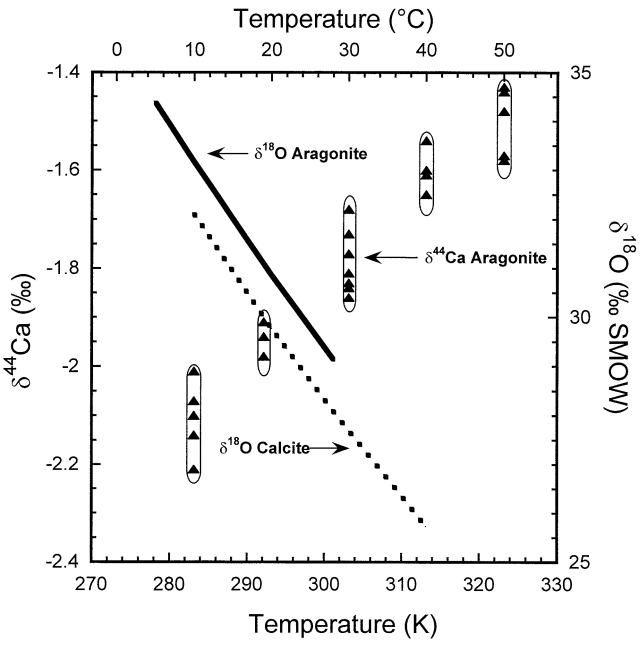

Fig. 2. Comparison of the experimentally determined temperature dependence for δ^{44}Ca of inorganic aragonite and the temperature dependence of δ^{18}O in isotopic equilibrium for aragonite (Böhm et al., 2000) and for calcite (Kim and O'Neil, 1997.)

bonding energies and, hence, are more stable than covalent bonds formed with lighter isotopes (O'Neil, 1986; O'Neil et al., 1969). As a consequence of the covalent bonding with C and H atoms, the δ^{18}O ratios of the dissolved carbonate species CO_2, HCO_3^-, and CO_3^{2-} always tend to be heavier than the δ^{18}O composition of the surrounding bulk solution (e.g., seawater). For example, at 19°C the isotope fractionation of H_2O versus $CO_{2(aq)}$, HCO_3^-, and solid $CaCO_3$ is ~58‰, 34‰, and 29‰, respectively (Zeebe, 1999).

In contrast, elements like Ca tend to form ionic rather than covalent bonds in carbonate crystals (O'Neil, 1986). Therefore, Ca isotope fractionation is only affected by kinetic isotope fractionation and not by equilibrium fractionation because no vibration bonding modes are active (O'Neil et al., 1969). In general, at fluid–solid interactions both kinetic and equilibrium fractionation processes are temperature-dependent. At lower temperatures, equilibrium fractionation tends to enrich the heavier isotope in the more stable molecules whereas kinetic fractionation tends to enrich the lighter isotopes in the product phase. Consequently, isotope systems like δ^{18}O controlled by equilibrium fractionation are an inverse function of temperature, whereas isotope systems like δ^{44}Ca, controlled by kinetic fractionation, are positively related to temperature (Fig. 3). Increasing temperature diminishes the isotope fractionation contrast between the reactants in the bulk solution and the product (e.g., $CaCO_3$).

4.2. Kinetic Effects on the Isotope Fractionation–Temperature Relation

It is generally accepted that diffusion across a liquid–solid boundary to and along a crystal growth surface is mass-depen-

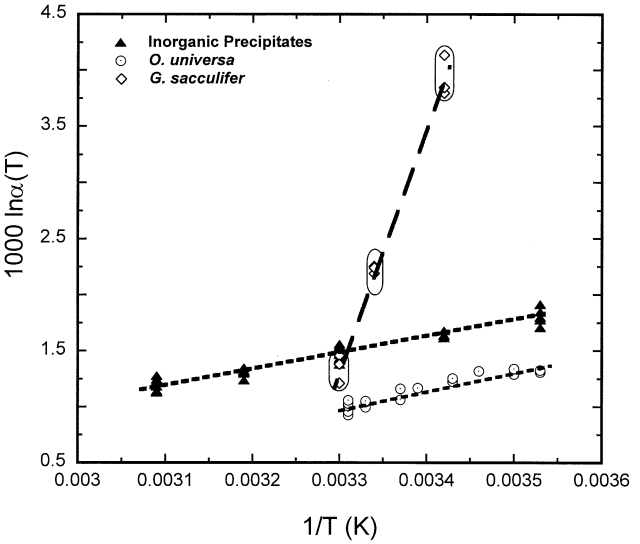

Fig. 3. The enrichment factor 1000 lnα(T) is shown as a function of the inverse temperature [$\alpha(T) = (^{44}Ca/^{40}Ca)_{bulk\ solution}/(^{44}Ca/^{40}Ca)_{carbonate}$]. Although there is a slight offset between *O. universa* and the inorganic precipitates, it can be seen that the slopes of the enrichment factors 1000 lnα(T) are quite similar. In contrast, the slope of the enrichment factor of *G. sacculifer* is steeper by a factor of 13 and 16, respectively.

Table 2. Initial values (α_0) and slopes (ζ) for the enrichment factor α(T).

	α_0	ζ
Precipitates	0.997	1.37
O. universa	0.996	1.64
G. sacculifer	0.932	21.6

α_0 and ζ values are calculated initial values and slopes for the enrichment factor $\alpha(T) = \alpha_0 \cdot \exp(-\zeta)$. The slope ζ corresponds to $E/k \cdot T$ (E = energy, k = Boltzman constant, T = absolute temperature).

dent because the diffusion velocities of the lighter isotopes are faster than those of the heavier isotopes. Therefore, the enrichment of the lighter isotope in the $CaCO_3$ crystal relative to the bulk solution as a function of temperature can be described by an enrichment factor α(T). Equations A1 and A2 in the appendix show that the slope of the enrichment factor α(T) is a function of the ratio of the mass difference (Δm) between the heavy and the light isotope and the reduced isotope mass (m). These equations clearly show that kinetic isotope fractionation is most efficient for low masses at low temperatures. For relatively high masses and high temperatures, the enrichment factor approaches unity as expected for kinetic isotope fractionation (see appendix).

These thermodynamic considerations can be used to identify processes responsible for our measured δ^{44}Ca data. In the case of an exclusive kinetic fractionation of ^{40}Ca and ^{44}Ca, it can be predicted that the slopes for α(T) of the precipitates and the two investigated foraminiferal species should be similar. From Table 2 it can be seen that the slopes of the enrichment factors for *O. universa* and the inorganic precipitates are similar. However, a major difference exists between inorganic precipitates, *O. universa* and *G. sacculifer*. The slope of α(T) for *G. sacculifer* is steeper by a factor of 13 relative to *O. universa* and a factor of 16 relative to the precipitates (Table 2).

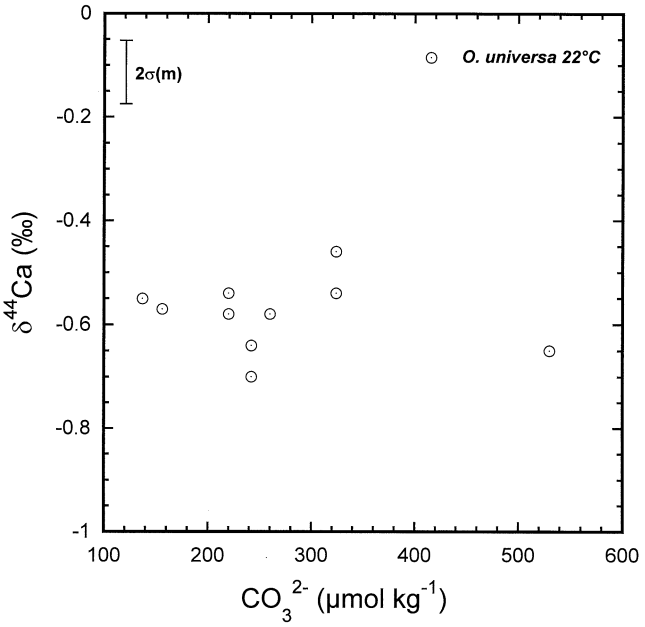

Fig. 4. The δ^{44}Ca values are plotted as a function of the $(CO_3)^{2-}$ concentration. Although the $(CO_3)^{2-}$ concentration has been varied by almost a factor of 4, there is no indication of a pH dependence of the δ^{44}Ca ratios in *O. universa.*

From Eqn. A2 it follows that the slope of the enrichment factor α(T) is controlled by the (Δm/m) ratio. Relatively low (Δm/m) ratios correspond to relatively shallow slopes for α(T) whereas relatively large (Δm/m) ratios correspond to steep slopes for α(T). The observation of shallower slopes for the inorganic precipitates and *O. universa* apparently indicates that Ca speciation with atomic masses much larger than pure Ca atoms (e.g., 40 and 44 amu) must control the diffusion velocity in *O. universa* and the inorganic precipitates. The similarity of the slopes of *O. universa* and the inorganic precipitates indicates that an inorganic or thermodynamic process has to be involved to explain their similarity. This process cannot be simple Rayleigh fractionation because the latter effect is closely related to equilibrium fractionation and not to kinetic isotope fractionation as is the case for the Ca isotope system. Furthermore, the difference in Ca isotope fractionation behavior between *O. universa* and *G. sacculifer* indicates that their specific $CaCO_3$ precipitation mechanisms must be considerably different. Thus, a combination of inorganic transport mechanisms and kinetically controlled biochemical calcification processes has to be involved to explain the observed phenomena. In the section below, we will first focus on a model for Ca^{2+} diffusion into a $CaCO_3$ crystal. Then, we will discuss different calcification models for *O. universa* and *G. sacculifer*.

From the assumption that Ca is diffusing as pure Ca^{2+}-ion in *G. sacculifer*, we can estimate from the different slopes of the enrichment factors that the apparent atomic mass of the diffusing species in *O. universa* and the inorganic precipitates correspond to a weight of $\sim$520 $\pm$ 60 and 640 $\pm$ 70 amu, respectively. Masses of several hundred amu cannot reflect the motion of a single Ca^{2+}-ion or any other known inorganic Ca species within *O. universa* and the inorganic precipitates. Such large masses usually reflect either organic molecules or metal complexes (e.g., Ca^{2+}-aquocomplexes, Bockris and Reddy, 1973; Langmuir, 1997). Most likely, the influence of large organic molecules is negligible for the inorganic precipitates. Therefore, we hypothesize that these calculated masses reflect the motion and diffusion of Ca^{2+}-ion complexes (Ca^{2+}-aquocomplex) in *O. universa* and the inorganic precipitates. From the calculated masses of $\sim$520 (*O. universa*) and 640 amu (precipitates), we calculate hydration numbers (the number of water molecules associated with a single Ca^{2+}-ion) of $\sim$27 $\pm$ 4 and 33 $\pm$ 5.

In general, ion complexes are dissolved species that exist because of the association of a cation with an anion or with neutral molecules like water (Langmuir, 1997). Most trace metals and many major elements are transported in water in complexed form. Estimates of the number of water molecules associated with each cation (hydration number) are difficult to obtain, and the results vary with the technique used for determination. Koneshan et al. (1998) calculated first shell hydration numbers of 4 water molecules associated with a lithium ion and 7 water molecules associated with a potassium ion. Hydration numbers increase with increasing ionic size, as in the sequence $Li^+ < Na^+ < K^+ < Rb^+ < Cs^+$.

Recent work suggests that the first hydration shell of a

Ca^{2+}-aquocomplex consists of 8 water molecules ($Ca[H_2O]_8^{2+}$, 184 amu) (Jalilehvand et al., 2001; Koneshan et al., 1998), although in earlier publications between 6 and 10 water molecules are reported (Kaufman Katz et al., 1996; Langmuir, 1997; Spångberg et al., 2000). Modeling and experimental results indicate a strongly bound, clearly defined inner hydration shell and a more weakly bound second shell (Jalilehvand et al., 2001; Koneshan et al., 1998). Molecules of the second shell are bound by hydrogen bondings to the water molecules of the first hydration shell. The number of waters that may occupy the second hydration sphere varies depending on the model selected from 11 to 18 (Jalilehvand et al., 2001). The concept of strongly bound first shell and weakly bound second shell molecules is also supported by the findings that the residence time of a water molecule in the first shell ($Ca[H_2O]_8^{2+}$) of a Ca^{2+}-aquocomplex is ~40 times longer than in the second shell. The residence times of water molecules in the second shell of a Ca^{2+} are in the same order of magnitude as the residence times of water molecules in the first shell of alkali cations (Koneshan et al., 1998).

An atomic mass around 520 amu (*O. universa*) is compatible with the maximum value for a hydration number of ~25 which has recently been reported by Spångberg et al. (2000), Jalilehvand et al. (2001), and Koneshan et al. (1998). Values of more than 600 amu (inorganic aragonite) exceed the empirically determined and accepted hydration number for a Ca^{2+}-aquocomplex. Apparently higher hydration numbers might be caused by additional complexation with anions. This is also appealing because the mineral surface is charged and the electrostatic repulsion is reduced by ion-pairing the hydrated cation.

For example, in seawater ~10% of the dissolved Ca^{2+} is bound to SO_4^{2-} forming a $CaSO_4^0 \cdot nH_2O$ complex (Byrne, 2002). However, in our experiments, the inorganic aragonite was precipitated from a sulfate-free solution. Therefore, at least for our inorganically precipitated aragonite, complexation with SO_4^{2-} can be ruled out. Other anions such as Cl^- or carbonate species may play a role in this case.

We note, that the hypothesized fractionation processes involving hydrated and dehydrated Ca^{2+}-ions presented here have not yet been tested by experiments. We therefore consider our interpretation preliminary pending future confirmation.

4.3. Ca^{2+} Transport and Fractionation in *O. universa* and *G. sacculifer*

To reconcile our $\delta^{44}Ca$ data, we suggest that the $\delta^{44}Ca$ fractionation involved is similar in *Orbulina* and inorganic aragonite although their calcification mechanisms are different. For *G. sacculifer*, a metabolic process is suggested that actively dehydrates the Ca^{2+}-aquocomplex before calcification. Differences between *G. sacculifer* and *O. universa* have already been reported concerning Ca storage within the cytoplasm (Ca pools). Anderson and Faber (1984) hypothesized that *G. sacculifer* stores significant amounts of Ca in its cytoplasm before deposition. In contrast, Lea et al. (1995) found little evidence for a substantial Ca pool in *O. universa*. Both observations are in accord with our $\delta^{44}Ca$ data because Ca storage requests enzymatically mediated Ca transport which is performed more favorably in dehydrated ionic form than in complexed form. In contrast, the absence of Ca storage in *O. universa* points to a calcification process closer to inorganic $CaCO_3$ precipitation.

Following a model for imperforate foraminifera originally presented by ter Kuile (1991), we propose for *O. universa* that seawater is incorporated into vesicles within the cytoplasm by the process of vacuolization. Precipitation of $CaCO_3$ needles (Hemleben et al., 1986) is then triggered in the vesicles either by actively increasing the pH in the vesicle or by the removal of calcium carbonate precipitation inhibiting ions like Mg^{2+} or PO_4^{3-} (Swart, 1983). In the vesicle, $^{44}Ca/^{40}Ca$ fractionation occurs during the formation of the amorphous carbonate $CaCO_3$ which closely resembles the precipitation of inorganic $CaCO_3$.

Following a model for perforate foraminifera (ter Kuile, 1991), we further propose that dehydration of the Ca^{2+}-aquocomplex occurs anywhere at the transition from seawater to the cytoplasm of *G. sacculifer*. Presumably, regulated cell membranes ("voltage operated Ca^{2+} channels" [VOC]) are involved with the dehydration of the Ca^{2+}-aquocomplex. It is well known that such Ca^{2+} VOCs show a high selectivity for Ca^{2+} and are more selective for Ca^{2+} by a factor of 1000 than for other cations such as Na^+ and K^+ (Aidley and Stanfield, 1996; Tsien and Tsien, 1990). After dehydration of the Ca^{2+}-aquocomplex by passing the channels, the pure Ca^{2+} ions become attached to transport enzymes within the cytoplasm (ter Kuile, 1991). Kinetic $^{44}Ca/^{40}Ca$ fractionation then occurs at the phase transition of the Ca ions from the channels to the transport enzymes and the adsorption onto their ligands. Ca is either stored in Ca pools (Anderson and Faber, 1984) or transported by these enzymes directly to the site of calcification (ter Kuile, 1991).

Although our working hypothesis presented here is able to reconcile the observation, and is in line with the aforementioned species-dependent biologic/metabolic processes, it is clear that further studies will have to investigate parameters such as varying precipitation rates, pH changes, or chemical composition of the culture solution.

5. SUMMARY AND CONCLUSIONS

The temperature-dependent fractionation characteristics of $\delta^{44}Ca$ and $\delta^{18}O$ are opposite because $\delta^{44}Ca$ ratios in $CaCO_3$ are controlled by kinetic isotope fractionation only.

The slope of the enrichment factor $\alpha(T)$ of the inorganic precipitates and *O. universa* reflects the occurrence, transport, and diffusion of Ca^{2+}-aquocomplexes in seawater. Our $\delta^{44}Ca$ data reveal the motion of heavy Ca^{2+}-aquocomplexes. These heavy complexes are less sensitive to temperature-dependent kinetic isotope fractionation than pure Ca^{2+}-ions.

Ca isotope fractionation in *G. sacculifer* indicates dehydration of the Ca^{2+}-aquocomplex and transport in its pure ionic form presumably during biologically mediated processes.

A major conclusion of this study is that the results for *G. sacculifer* cannot be generalized to other species. For paleoceanographic applications it will be necessary to carefully study different species to elucidate their response to temperature as well as to other environmental influences.

Acknowledgments—This study is supported by a grant of the "Deutsche Forschungsgemeinschaft (DFG)" to A. Eisenhauer (Ei272/12-1, CAE-

SAR). The U.S. National Science Foundation supported this study with grants to H. J. Spero (OCE-9729203) and to D. W. Lea (OCE-9729327). Ca isotope work in Bern (Switzerland) is supported by SNF grant 21-61644 to Th. F. Nägler. H. J. Spero acknowledges the Hanse Institute for Advanced Studies, Delmenhorst, Germany for fellowship support. We also thank the research staff of the Wrigley Institute for Environmental Studies and the Isla Magueyes Marine Laboratory, Puerto Rico for assistance in the field. We thank R. Zeebe for helpful comment on earlier versions of the manuscript. In particular, we appreciate the help of D. R. Cole, A. Paytan, and T. Esat who significantly helped to improve the manuscript by constructive comments and helpful suggestions.

Associate editor: D. Cole

REFERENCES

Aidley D. J. and Stanfield P. R. (1996) *Ion Channels*. Cambridge University Press.

Anderson O.R. and Faber W.W. Jr (1984) An estimation of calcium carbonate deposition rate in a planktonic foraminifer Globigerinoides sacculifer using ^{45}Ca as a tracer: A recommended procedure for improved accuracy. *J. Foraminiferal Res.* **14**(4), 303–308.

Arp G., Reimer A., and Reitner J. (2001) Photosynthesis-induced biofilm calcification and calcium concentrations in phaerozoic oceans. *Science* **292,** 1701–1704.

Bigeleisen J. and Mayer M. G. (1947) Calculation of equilibrium constants for isotopic exchange reactions. *J. Chem. Phys.* **15,** 261–267.

Bockris J. O. and Reddy A. K. N. (1973) *Modern Electrochemistry*. Plenum Press.

Böhm F., Joachimski M. M., Dullo W.-C., Eisenhauer A., Lehnert H., Reitner J., and Wörheide G. (2000) Oxygen isotope fractionation in marine aragonite of coralline sponges. *Geochim. Cosmochim. Acta* **64**(10), 1695–1703.

Byrne R. H. (2002) Inorganic speciation of dissolved elements in seawater: The influence of pH on concentration ratios. *Geochem. Trans.* **3**(2), 11–16.

Compston W. and Oversby V. (1969) Lead isotopic analysis using a double spike. *J. Geophys. Res.* **74**(17), 4338–4348.

Degens E. T. (1979) Why do organism calcify? *Chem. Geol.* **25,** 257–269.

De La Rocha C. L. and DePaolo D. J. (2000) Isotopic evidence for variations in the marine calcium cycle over the Cenozoic. *Science* **289,** 1176–1178.

Dietzel M. and Usdowski E. (1996) Coprecipitation of Ni^{2+}, Co^{2+}, and Mn^{2+} with galena and covellite, and of Sr^{2+} with calcite during crystallization via diffusion of H_2S and CO_2 through polyethylene at 20°C: Power law and Nernst law control of trace elements partitioning. *Chem. Geol.* **131,** 55–65.

Hemleben C., Anderson O. R., Berthold W. and Spindler M. (1986) Calcification and chamber formation in foraminifera: A brief overview. In *Biomineralization in Lower Plants and Animals* (eds. B. S. C. Leadbeater and R. Riding), pp. 237-249. The Systematics Association.

Heumann K. G., Klöppel H., and Sigl G. (1982) Inversion der Calcium-Isotopenseparation an einem Ionenaustauscher durch Veränderung der LiCl-Elektrolytkonzentration. *Z. Naturforsch.* **37b,** 786–787.

Heumann K. G. and Lieser K. H. (1972) Untersuchung von Calciumisotopieeffekten bei heterogenen Austauschgleichgewichten. *Z. Naturforsch.* **27b**(2), 126–133.

Heumann K. G., Lieser K. H., and Elias H. (1970) Difficulties in measuring the isotopic abundances of calcium with a mass spectrometer. In *Recent Developments in Mass Spectroscopy* (eds. K. Ogata and T. Hayakawa), pp. 457-459. University of Tokyo Press.

Heuser A., Eisenhauer A., Gussone N., Bock B., Hansen B. T., and Nägler T. F. (2002) Measurement of calcium isotopes ($\delta^{44}Ca$) using a multicollector TIMS technique. *Int. J. Mass Spec.* **220,** 387–399.

Jalilehvand F., Spångberg D., Lindqvist-Reis P., Hermansson K., Persson I., and Sandström M. (2001) Hydration of the calcium ion: An EXAFS, large-angle X-ray scattering, and molecular dynamics simulation study. *J. Am. Chem. Soc.* **123,** 431–441.

Kaufman Katz A., Glusker J. P., Beebe S. A., and Bock C. W. (1996) Calcium ion coordination: A comparison with that of beryllium, magnesium, and zinc. *J. Am. Chem. Soc.* **118,** 5752–5763.

Kempe S. and Degens E. T. (1985) An early soda ocean? *Chem. Geol.* **53,** 95–108.

Kim S.-T. and O'Neil J. R. (1997) Equilibrium and nonequilibrium oxygen isotope effects in synthetic carbonates. *Geochim. Cosmochim. Acta* **61,** 3461–3475.

Koneshan S., Rasaiah J. C., Lynden-Bell R. M., and Lee S. H. (1998) Solvent structure, dynamics, and ion mobility in aqueous solutions at 25°C. *J. Phys. Chem. B* **102,** 4193–4204.

Langmuir D. *Aqueous Environmental Geochemistry*. Prentice Hall.

Lea D. W., Martin P. A., Chan D. A., and Spero H. J. (1995) Calcium uptake and calcification rate in the planktonic foraminifer Orbulina universa. *J. Foraminiferal Res.* **25**(1), 14–23.

Lea D. W., Pak D. K., and Spero H. J. (2000) Climate impact of late quaternary equatorial Pacific sea surface temperature variations. *Science* **289**(5485), 1719–1724.

Nägler T., Eisenhauer A., Müller A., Hemleben C., and Kramers J. (2000) The $\delta^{44}Ca$-isotopes: New powerful tool for reconstruction of past sea surface temperatures. *Geochem. Geophys. Geosyst.* **1**.(doi: 10.10292000GC000091).

O'Neil J. R., Clayton R. N., and Mayeda T. K. (1969) Oxygen isotope fractionation in divalent metal carbonates. *J. Chem. Phys.* **51**(12), 5547–5558.

O'Neil J. R. (1986) Theoretical and experimental aspects of isotopic fractionation. In *Reviews of Mineralogy. Stable Isotopes in High Temperature Geological Processes*, 16 (eds. J. W. Valley, J. R. O'Neil, and H. P. Taylor), pp. 561-570. Mineralogical Society of America.

Russell W. A., Papanastassiou D. A., and Tombrello T. A. (1978) Ca isotope fractionation on the Earth and other solar system materials. *Geochim. Cosmochim. Acta* **42,** 1075–1090.

Skulan J. L., DePaolo D. J., and Owens T. L. (1997) Biological control of calcium isotopic abundances in the global calcium cycle. *Geochim. Cosmochim. Acta* **61,** 2505–2510.

Skulan J. and DePaolo D. J. (1999) Calcium isotope fractionation between soft and mineralized tissues as a monitor of calcium use in vertebrates. *Biochemistry* **96**(24), 13709–13713.

Spångberg D., Hermansson K., Lindqvist-Reis P., Jalilehvand F., Sandström M., and Persson I. J. (2000) Phys. *Chem. B* **104,** 10467–10472.

Spero H. J. (1998) Life history and stable isotope geochemistry of planktonic foraminfera. In *Isotope Paleobiology and Paleoecology, Paleontological Society Papers*, Vol. 4 (eds. R. D. Norris and R. M. Corfield), Paleontological Society, pp. 7–36.

Spero H. J., Bijma J., Lea D. W., and Bemis B. E. (1997) Effect of seawater carbonate concentration on planktonic foraminiferal carbon and oxygen isotopes. *Nature* **390,** 497–500.

Stahl W. and Wendt L. (1968) Fractionation of calcium isotopes in carbonate precipitation. *Earth Planet. Sci. Lett.* **5,** 184–186.

Stanley S. M. and Hardie L. A. (1998) Secular oscillations in the carbonate mineralogy of reef-building and sediment-producing organisms driven by tectonically forced shifts in seawater chemistry. *Palaeogeogr. Palaeocl. Palaeoecol.* **144,** 3–19.

Swart P. K. (1983) Carbon and oxygen isotope fractionation in scleractinian corals: A review. *Earth. Sci. Rev.* **19,** 51–80.

ter Kuile B. T. (1991) Mechanisms for calcification and carbon cycling in algal symbiont-bearing foraminifera. In *Biology of Foraminifera* (eds. J. L. Lee and O. R. Anderson), pp. 74–89. Academic Press.

Tsien R. W. and Tsien R. Y. (1990) Calcium channels, stores, and oscillations. *Ann. Rev. Cell Biol.* **6,** 715–760.

Urey H. C. (1947) The thermodynamic properties of isotopic substances. J. Chem. Soc. 562–581.

Wallmann K. (2001) Controls on the Cretaceous and Cenozoic evolution of seawater composition, atmospheric CO_2 and climate. *Geochim. Cosmochim. Acta* **65**(18), 3005–3025.

Williams R. J. P. (1974) Calcium ions: Their ligands and their function. *Biochemical Society Symposia* **39,** 133–138.

Williams R. J. P. (1989) Calcium and cell steady states. In *Calcium Binding Proteins in Normal and Transformed Cells* (eds. R. Pochet, D. E. M. Lawson, and C. W. Heizmann), pp. 7–16. Plenum.

Zeebe R. E. (1999) An explanation of the effect of seawater carbonate concentration on foraminiferal oxygen isotopes. *Geochim. Cosmochim. Acta* **63,** 2001–2007.

Zeebe R. E. and Wolf-Gladrow D. A. (2001). *CO_2 in Seawater: Equilibrium, Kinetics, Isotopes.* Elsevier.

Zhu P. and MacDougall J. D. (1998) Calcium isotopes in the marine environment and the oceanic calcium cycle. *Geochim. Cosmochim. Acta* **62**(10), 1691–1698.

APPENDIX

The enrichment factor α(T) is described by a partitioning function (Eqn. A1) where ΔE is the difference of the kinetic energy (E_{kin}) between the heavy and the light isotope.

$$\alpha(T) \approx \alpha_0 \cdot e^{\frac{-\Delta E}{E}};\ E_{kin} = \frac{3}{2} \cdot \mathrm{k} \cdot \mathrm{T} \text{ and } \Delta\mathrm{E} \approx E_{kin} \cdot \frac{\Delta \mathrm{m}}{\mathrm{m}} \quad \text{(A1)}$$

It follows:

$$\alpha(T) = \alpha_0 \cdot e^{-\frac{2 \cdot E_{kin}}{3 \cdot k} \cdot \frac{\Delta m}{m} \cdot \frac{1}{T}} \quad \text{(A2)}$$

where α(T) = $(^{44}Ca/^{40}Ca)_{fluid}/(^{44}Ca/^{40}Ca)_{solid}$, E_{kin} = kinetic energy, m = reduced atomic mass for the light and heavy isotope, k = Boltzman constant ($1.38 \cdot 10^{-23}$ J/K), and T = absolute temperature in Kelvin (K).